Molecular Cell, Vol. 15, 199–208, July 23, 2004, Copyright ©2004 by Cell Press

Molecular Architecture of the *S. cerevisiae* SAGA Complex

Pei-Yun Jenny Wu,[3] Christine Ruhlmann,[1,2] Fred Winston,[3] and Patrick Schultz[1,2,*]
[1]Institut de Génétique et
de Biologie Moléculaire et Cellulaire
CNRS/INSERM/ULP
1, rue Laurent Fries, BP163
67404 Illkirch
France
[2]Ecole Supérieure de Biotechnologie de Strasbourg
Pôle API
1, rue Sébastien Brandt
67400 Illkirch
France
[3]Department of Genetics
Harvard Medical School
Boston, Massachusetts 02115

Summary

The *Saccharomyces cerevisiae* SAGA complex is a multifunctional coactivator that regulates transcription by RNA polymerase II. The 3D structure of SAGA, revealed by electron microscopy, is formed by five modular domains and shows a high degree of structural conservation to human TFTC, reflecting their related subunit composition. The positions of several SAGA subunits were mapped by immunolabeling and by analysis of mutant complexes. The Taf (TBP-associated factor) subunits, shared with TFIID, occupy a central region in SAGA and form a similar structure in both complexes. The locations of two histone fold-containing core subunits, Spt7 and Ada1, are consistent with their role in providing a SAGA-specific interface with the Tafs. Three components that perform distinct regulatory functions, Spt3, Gcn5, and Tra1, are spatially separated, underscoring the modular nature of the complex. Our data provide insights into the molecular architecture of SAGA and imply a functional organization to the complex.

Introduction

Transcription initiation by RNA polymerase II is a highly regulated process that requires the coordinated activities of a large number of factors. One important and conserved class of factors is coactivators, multiprotein complexes that are recruited to promoters by gene-specific activators to facilitate transcription initiation. Coactivators have been shown to function by several distinct mechanisms to integrate different functions required for regulated gene expression, such as nucleosome remodeling and recruitment of general transcription factors (reviewed in Cosma, 2002; Roth et al., 2001).

One coactivator that has been extensively studied by both genetic and biochemical approaches is the *S. cerevisiae* SAGA complex. SAGA is a 1.8 MDa coactivator containing approximately 14 polypeptides that has been shown to modulate the transcription of numerous genes. To function as a transcriptional coactivator, SAGA utilizes the activities of its many subunits. First, SAGA modifies histones by acetylation, as mediated by the Gcn5 catalytic subunit, and its activity is modulated by the associated proteins Ada2 and Ada3 (Balasubramanian et al., 2001; Brownell et al., 1996; Grant et al., 1997; Sterner et al., 2002). In addition to its enzymatic activities, SAGA can regulate the TBP-TATA interaction through the Spt3 and Spt8 subunits at particular promoters, including *GAL1*, *HIS3*, *PHO5*, and *HO* (Barbaric et al., 2003; Belotserkovskaya et al., 2000; Bhaumik and Green, 2001; Eisenmann et al., 1992; Larschan and Winston, 2001; Yu et al., 2003). Finally, interactions between SAGA and activators have been shown to involve Tra1 and several histone fold-containing subunits, including Ada1, Taf6, and Taf12 (Bhaumik and Green, 2004; Brown et al., 2001; Hall and Struhl, 2002; Klein et al., 2003).

The structural integrity of SAGA requires two additional groups of proteins. The Spt7, Spt20, and Ada1 subunits function as SAGA core components, and mutant strains that do not express any one of these subunits lack intact SAGA complex and exhibit severe phenotypes (Grant et al., 1997; Horiuchi et al., 1997; Roberts and Winston, 1997; Sterner et al., 1999; Wu and Winston, 2002). Further biochemical characterization suggests that Spt7 plays a key role in SAGA assembly and in maintaining normal levels of SAGA (Wu and Winston, 2002). The second group consists of a subset of the Tafs (Taf5, Taf6, Taf9, Taf10, and Taf12), essential proteins initially identified as components of the TFIID general transcription factor (Grant et al., 1998a). Mutations in *TAF5*, *TAF10*, and *TAF12* affect SAGA composition and integrity, indicating the importance of these proteins for SAGA structure (Durso et al., 2001; Grant et al., 1998a; Kirschner et al., 2002).

Recent studies have begun to elucidate the subunit interactions within SAGA. Two Taf subunits in SAGA, Taf10 and Taf12, have been shown to associate directly through their histone fold domains with the SAGA-specific core components Spt7 and Ada1, respectively (Gangloff et al., 2000, 2001). Experiments to reconstitute subunit interactions between Tafs and their partners using recombinant proteins have demonstrated that the heterodimer pairs Ada1-Taf12 and Taf6-Taf9 form an octameric complex (Selleck et al., 2001). Characterization of a number of SAGA subunit mutants has also contributed information on their contacts in SAGA. Examination of SAGA purified from *taf10* mutants suggests that Taf10 can associate with both Spt7 and Ada2 (Kirschner et al., 2002). Similarly, Taf5 mutants are significantly reduced in their ability to interact with Spt7, Ada1, and Ada3 (Durso et al., 2001). Biochemical analysis of mutant SAGA complexes has also yielded a general picture of the structural requirements for different subunits in SAGA. Deletion of the core components Spt20 and Ada1 dramatically alters the composition of the complex, demonstrating their important role in SAGA

*Correspondence: patrick.schultz@igbmc.u-strasbg.fr

structure and suggesting a central location in SAGA (Wu and Winston, 2002). The absence of subunits that are not essential for maintaining complex integrity, such as Spt3 and Gcn5, does not affect the association of any other proteins within SAGA, suggesting a peripheral location in the complex.

Some insight into SAGA architecture was provided by the determination of the structures of the TFTC and TFIID transcription complexes by electron microscopy. The TFTC, PCAF, and STAGA complexes are human homologs of SAGA that contain many of the same subunits (Brand et al., 1999b; Martinez et al., 1998; Martinez et al., 2001; Ogryzko et al., 1998). TFTC forms an elongated particle approximately 27 × 16 nm in size composed of five domains (Brand et al., 1999a). However, the structural homology between TFTC and SAGA remains to be demonstrated, and more importantly, the organization of subunits within these coactivators is unknown. Some information about the organization of SAGA may be inferred from studies of TFIID. The structure of *S. cerevisiae* TFIID is composed of three major lobes and resembles a molecular clamp (Leurent et al., 2002, 2004). Immunolabeling experiments demonstrated that Tafs containing histone fold domains are present in two locations and confirmed that the previously characterized heterodimer pairs are present in the native structure. As SAGA contains several Tafs (Grant et al., 1998a), it is important to determine whether this subunit stoichiometry is preserved and whether TFIID and SAGA share an underlying organization based on a Taf substructure.

To investigate the molecular organization of SAGA, we have determined the three-dimensional (3D) structure of SAGA and characterized the positions of many of its subunits by electron microscopy. Our results show that SAGA is similar in size and structure to its human counterpart, TFTC, reflecting conservation in function as well as subunit composition. Localization of the Taf subunits in SAGA suggests a central structure that may form a scaffold on which SAGA-specific proteins assemble. Part of the Taf interface consists of core components of the complex, Spt7 and Ada1, which interact with the Tafs through their histone fold domains. Detailed mapping of SAGA subunits that provide key functions in transcriptional control, such as Spt3, Tra1, and Gcn5, demonstrate their spatial separation in distinct structural lobes.

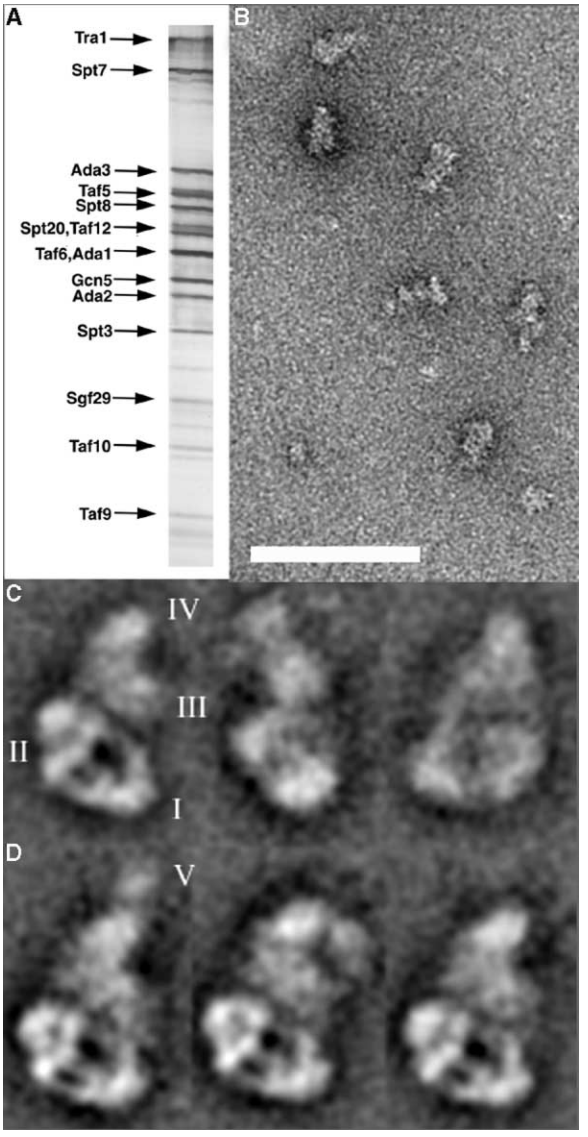

Figure 1. Electron Microscopy and Image Analysis of the *S. cerevisiae* SAGA Complex

(A) TAP-purified SAGA from an Spt7-TAP-tagged, otherwise wild-type strain (FY2031) was prepared, run on a 5%–20% SDS-PAGE gel, and silver stained.

(B) Electron micrograph of SAGA molecules adsorbed on a carbon film and negatively stained with uranyl acetate, showing the homogeneity in size and the dispersion of the complexes.

(C) Representative SAGA views. The three views correspond to different orientations of the molecule. In the view shown in the left panel, four domains are revealed and are identified as I–IV.

(D) Three views of SAGA that reveal a fifth domain (labeled V) that can adopt various positions (compare the left and the central panel) or can be absent (right panel). The bar represents 100 nm in (B) and 20 nm in (C) and (D).

Results

A Three-Dimensional Model of the *S. cerevisiae* SAGA Complex

The *S. cerev*isiae SAGA complex was affinity purified on protein A and calmodulin columns via a C-terminal TAP tag on the Spt7 subunit, and characterized as previously described (Figure 1A) (Wu and Winston, 2002). This preparation of SAGA possesses histone acetyltransferase activity and can be specifically recruited to a nucleosomal array by the Gal4-VP16 activator in vitro (data not shown). When viewed by electron microscopy, about two-thirds of the complexes appeared as elongated particles 27 × 18 nm in size (Figure 1B). Smaller particles that could represent either degradation products or contaminants were also observed and were not further analyzed. The elongated particles were observed reproducibly in several different preparations and were found to be absent from *ada1*Δ mutants, indicating that they correspond to the SAGA molecules. A total of 6041 molecular images were recorded and numerically analyzed to obtain characteristic views of the particle. In

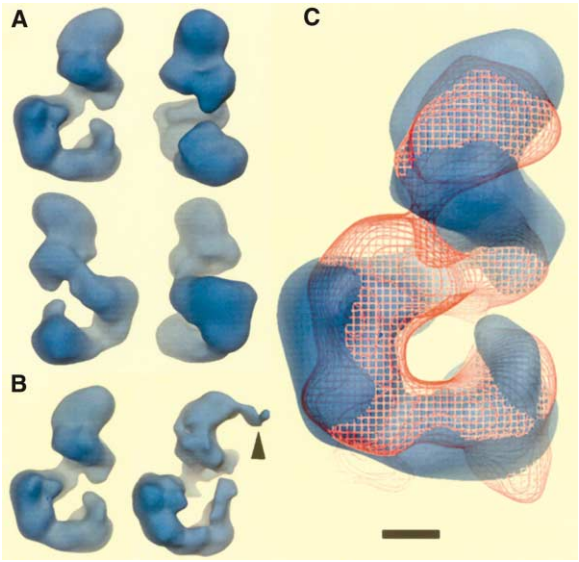

Figure 2. Three-Dimensional Model of the SAGA Complex and Comparison with the Human TFTC Complex

(A) Surface representation of the 3D reconstruction of SAGA at a resolution of approximately 3.1 nm. The model is turned around a vertical axis by equally spaced increments of 90°.

(B) Surface representation of the average SAGA model (left) and a model derived from a subpopulation of images in which the flexible domain V was present in a fixed position (right). However, due to the residual flexibility of this apical region, the size of domain V (arrowhead) is smaller than expected.

(C) Alignment and superposition of the SAGA model (blue) with the previously determined human TFTC model (red) (Brand et al., 1999a). The bar represents 10 nm in (A) and (B) and 3.7 nm in (C).

several views, SAGA appears to be composed of four domains, 7–10 nm in size (labeled I–IV in Figure 1C), linked together in an almost linear arrangement. Upon closer inspection of a characteristic view, an additional protein domain V was detected at the tip of the complex, in contact with domain IV (Figure 1D). Variance analysis of this region showed that this domain is flexible since it was found in different positions with respect to domains I–IV (Figure 1D, compare left and central panels). Furthermore, domain V was not visible in about 35% of the molecular images, suggesting that it may be transiently attached to the SAGA complex (Figure 1D, right panel).

The SAGA views reveal striking similarities with the previously analyzed TFTC complex, allowing for the use of the 3D model of TFTC for angular assignment. A total of 118 different views of the SAGA complex were identified, and the angular distribution of the views showed that they form a tomographic series around the long axis of the molecule (data not shown). The resolution tests gave values of 3.4 and 2.8 nm for the 0.5 FSC and the 3σ criteria, respectively (see Experimental Procedures). The density threshold was set to delimit a volume of 1900 kDa, consistent with the mass of the complex determined by gel filtration (Grant et al., 1997). SAGA is composed of four major domains that form a particle 27 $\times$ 17 $\times$ 13 nm in size (Figure 2A). The two largest domains, I and II, 10 $\times$ 11 $\times$ 8 nm and 12 $\times$ 9 $\times$ 10 nm in size, respectively, show considerable internal details. Domain III (8 $\times$ 8 $\times$ 10 nm) is connected to domain II through a thin linker and to domain IV (9 $\times$ 13 $\times$ 9 nm). Two large clefts are present in the structure of SAGA, formed by domains I, II, and III for one and by domains II, III, and IV for the second. To prevent the vanishing of the flexible domain V upon averaging, a model was generated after selection of the complexes in which domain V had a similar position. Three cycles of reconstruction and sorting of the particles on the basis of their similarity with the model showing the additional density were used to recover domain V from background (Figure 2B, right panel).

The overlay of the previously determined 3D structure of human TFTC (Brand et al., 1999a) on the envelope of SAGA shows the conservation in size and overall shape of the two complexes which reflects their functional homology and related subunit composition (Figure 2C). Major differences were observed in the positions of protein domains such as domain V in SAGA or a detachable part connected to the corresponding domain II in TFTC. These differences reflect the presence of unique subunits in either TFTC or SAGA and may indicate their ability to carry out distinct but related functions.

Mapping of the Taf Subcomplex Common to SAGA and TFIID

SAGA and TFIID share five subunits (Taf5, Taf6, Taf9, Taf10, and Taf12) that are likely to form a similar substructure in both complexes, and antibodies were used here to examine the arrangement of three Tafs in SAGA. Purified SAGA was incubated with a Taf6-specific polyclonal antibody and the analysis of 509 molecules identified two distinct labeled sites in view 4, in domains II and III (Table 1 and Figure 3A). These results suggest that Taf6 is present in two copies in SAGA, similar to what was determined for yTFIID, where all histone fold domain (HFD) Tafs were found to be present in two locations (Leurent et al., 2002). The position of Taf5, a Taf without a HFD, was determined using a monoclonal antibody directed against the N-terminal part of the protein. This analysis showed that the antibody binds to domain III (Table 1 and Figure 3C). Finally, for Taf10, the antibodies were found to bind to the central part of the molecules in view 3, a result confirmed for other orientations of the particle. Within this specific region, two antibody binding sites were detected, one in domain III and one in domain II. For each antibody binding site an average view was produced and a density difference map was calculated with the corresponding unlabeled view and was contoured at a 3σ significance threshold (Figure 3A). These findings suggest that Taf10 is present in two copies within SAGA, as was previously found for TFIID (Leurent et al., 2002). However, due to the pronounced symmetry of view 3 and the symmetric position of the two binding sites, it cannot be excluded that the two labeled sites correspond to the same location.

The spatial distribution of Taf5, Taf6, and Taf10 was found to be similar in SAGA and in TFIID (Figure 3D). The positions of Taf5 and Taf6 were used as anchor points to align the 3D models of TFIID and SAGA (Figure 3E). This alignment shows that the TFIID clamp fits into the cleft formed by the SAGA domains II, III, and IV. However, major densities in TFIID, particularly lobe B,

Table 1. Labeling Statistics

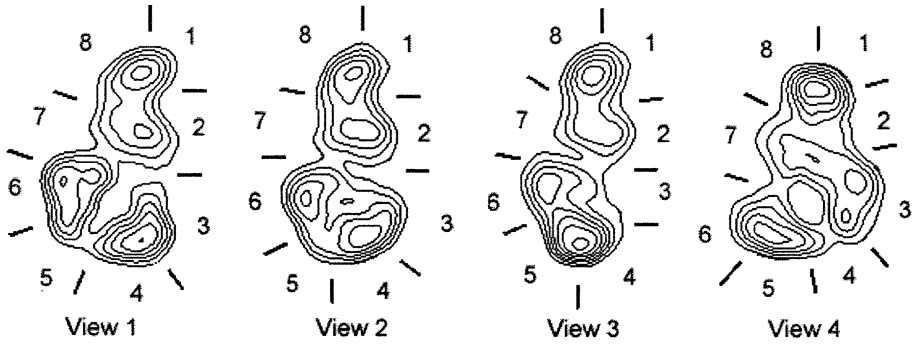

Labeled Subunit	Number of Images n1	View	n2	Sector 1	2	3	4	5	6	7	8
Taf10	582	3	125	0.2	*18.5*	0.7	0.2	0.7	*11.8*	0.7	1.0
Taf 6	509	4	89	1.0	1.0	*7.3*	0.4	*4.5*	1.2	1.2	0.1
Taf5	456	2	159	0.5	1.2	1.0	0.9	1.1	0.8	*7.1*	0.5
Spt7	654	1	170	1.3	*3.0*	0.3	0.8	0.6	1.9	0.6	0.5
Ada1	560	1	111	0.9	1.7	0.6	0.6	0.6	0.6	*9.9*	*11.4*
		2	246	0.9	0.6	0.3	2.2	1.6	0.2	*3.5*	*6.9*
Tra1	809	1	119	1.9	1.0	*11.9*	1.0	0.2	0.2	0.4	0.2
		2	39	0.4	0.4	*10.6*	0.6	1.4	1.5	0.4	0.6
Spt20	1399	1	244	1.9	0.7	0.5	0.8	0.1	0.8	1.0	*4.1*
		3	212	1.9	0.9	0.3	1.2	1.0	0.7	0.9	*3.9*
Spt3	803	1	136	*15.1*	0.3	0.7	0.3	0.3	1.2	0.3	0.3
Gcn5	1676	1	126	0.4	*4.8*	1.8	0.4	0.1	0.1	1.5	1.4
		2	112	0.6	*7.4*	0.9	0.9	0.9	0.4	1.7	0.2
		3	203	0.6	*5.3*	1.0	1.0	0.1	1.1	1.0	1.1

The upper panel shows the four major views analyzed and their division into eight sectors used to determine labeling specificity. For each antibody used to detect the position of a SAGA subunit, the table shows the number of recorded labeled particles (n1), the particular view analyzed (view), and the number of images corresponding to the analyzed view (n2). The values reported for each sector represent deviations from the average binding frequency (in sigma folds). Italic characters represent values higher than 3σ.

fall outside of the SAGA envelope, and conversely, SAGA domains I and V are absent in TFIID. These differences reflect the contributions made by specific subunits.

Localization of the Histone Fold Domain-Containing Subunits Ada1 and Spt7

In SAGA, biochemical characterization, using recombinant purified proteins, has demonstrated the formation of an octameric complex comprised of Ada1, Taf6, Taf9, and Taf12 (Selleck et al., 2001). Other studies have shown that two histone fold domain (HFD)-containing Tafs, Taf10, and Taf12, interact with two other SAGA-specific HFD-containing proteins, Spt7 and Ada1, respectively (Gangloff et al., 2000, 2001; Reese et al., 2000). In order to investigate whether the Taf10-Spt7 and Taf12-Ada1 interactions are plausible within the SAGA complex, the positions of Spt7 and Ada1 were determined by different labeling approaches. In addition, the structure of an *ada1*Δ mutant SAGA was characterized.

Two distinct methods were employed to position Spt7 within SAGA. First, the Spt7-CBP C-terminal fusion, the form of Spt7 in SAGA in the purified preparations used for these studies, was used to bind streptavidin-coupled, biotinylated calmodulin in the presence of an excess of calcium chloride (see Experimental Procedures). After incubation with this probe, 926 images of SAGA were collected, and image analysis showed a new protein domain, consistent with the size of streptavidin, in the labeled complexes (Figure 4A, left panel). This observation was made for several independent views and is consistent with a unique 3D location of Spt7 in domain III. The second approach utilized an HA-specific antibody to probe the position of an HA tag fused to the N terminus of Spt7. Analysis of 654 antibody-labeled complexes revealed that the probe specifically bound domain III, in agreement with the results obtained with the calmodulin labeling (Table 1 and Figure 4A, central panel). Taken together, these results show that Spt7 maps near the Taf subassembly, in close proximity to Taf10, and that Spt7 is present as a single copy in SAGA.

To map the position of Ada1 in SAGA, we used an Ada1-specific polyclonal antibody and two distinct SAGA views were analyzed (Table 1 and Figure 4B, upper and lower panels, respectively). In both orientations of SAGA, the antibodies bound to two distinct sites, one in domain II and one between domains III and IV. A small fraction of complexes was labeled twice by the same antibody (Figure 4B, upper right panel). These observations indicate that there are two copies of Ada1 in SAGA and that both reside proximal to the Taf subunits. The Ada1 subunits map in the domains in which the two Taf12 subunits are predicted to be located based on their arrangement in TFIID relative to other Tafs (Figure

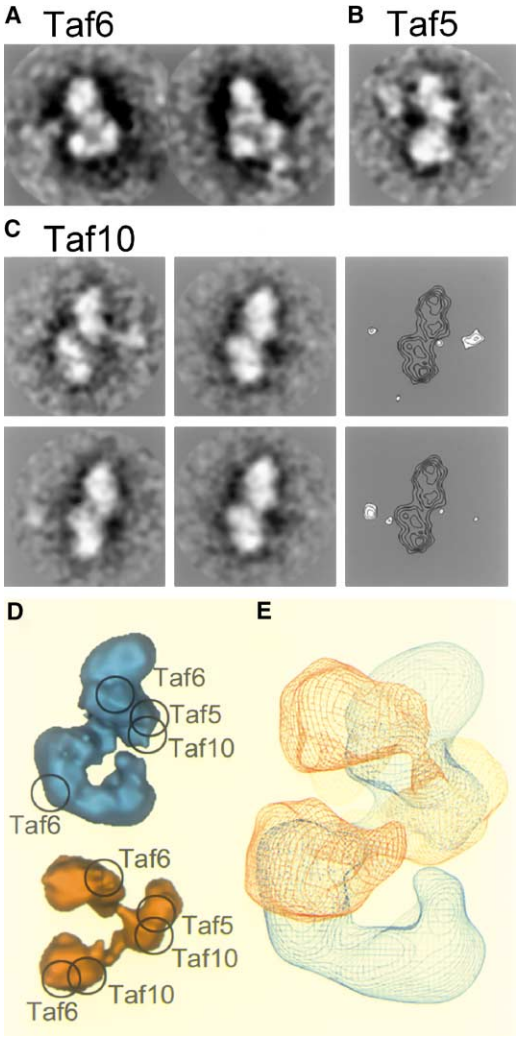

Figure 3. Immunolabeling of the Taf Subunits Shared by SAGA and TFIID

(A) Mapping of the interaction sites of Taf6-specific antibodies on a particular SAGA view. Two specific labeled sites are identified in domains III (left panel) and II (right panel) on the average labeled views.

(B) Average image showing that the labeling by antibodies directed against the N terminus of Taf5 is located in domain III of SAGA.

(C) Mapping of the Taf10-specific antibody binding sites at the outer contour of a characteristic four-domain SAGA view. The left panels show average images of SAGA molecules labeled in domain III (top) or II (bottom), the central panels show the corresponding unlabeled view, and the right panels show the density difference map between the labeled and the unlabeled views. The difference is contoured at a 3σ significance threshold and is overlaid to isodensity contours of the unlabeled view.

(D) Schematic representation of the positions of Taf5, Taf6, and Taf10 on the SAGA model (turquoise) or on the model of TFIID (orange, from Leurent et al., 2002) indicating that the spatial distribution of the common Tafs is comparable.

(E) Orientation of TFIID (orange) and SAGA (turquoise) that maximizes the fit between the distribution of the common Tafs in both complexes. The overlapping region is likely to contain the shared substructure formed by the five shared Tafs.

6), which is consistent with the ability of Ada1 and Taf12 to form specific heterodimers.

Previous biochemical analysis showed that in an *ada1*Δ mutant, a SAGA subcomplex forms in which the subunit content is drastically reduced (Wu and Winston, 2002). The mutant complex is most notably missing Tra1, Spt3, Taf12, Sgf29, and Ada3 (Figure 4C). When observed by electron microscopy, the purified particles appear significantly smaller than the wild-type SAGA particles, confirming that the integrity of the complex is strongly affected by the absence of Ada1 (Figure 4D). The analysis of 2478 molecular images revealed characteristic views of the *ada1*Δ mutant (Figure 4E). The 3D model derived from 63 different views shows that the particle is composed of three distinct domains (Figure 4G). The 3D model was reprojected to illustrate the similarity between the calculated model and the original class averages (compare Figures 4E and 4F). The 3D model of the *ada1*Δ particles was mapped onto the model of the wild-type complex, using the positions of the two Ada1 subunits determined above as boundaries. The best fit between the two models indicates that the *ada1*Δ mutant particle is centered on lobe III of SAGA and occupies part of lobes II and IV (Figure 4H). This positioning is consistent with our immunolocalization of both Tra1 and Spt3, both of which are predicted to be absent in the *ada1*Δ SAGA mutant, and this is confirmed by the biochemical characterization.

Localization of Tra1 and Spt20

The largest subunit in SAGA, the 400 kDa Tra1 protein, is a component of multiple histone acetyltransferase complexes (Allard et al., 1999; Grant et al., 1998b, 1999; Saleh et al., 1998). Previous studies have demonstrated that it can interact directly with activators known to require SAGA for regulating transcription (Bhaumik and Green, 2004; Brown et al., 2001). Tra1 was mapped using a strain in which it was myc-tagged at the N terminus (Hall and Struhl, 2002). The analysis of 809 complexes labeled with an anti-myc antibody showed, in two distinct views, that Tra1 was located within domain I (Table 1 and Figure 5A). Because of the size of Tra1, it is unclear if the protein resides solely in domain I or extends further throughout the structure. The position of Spt20 was mapped with a polyclonal antibody that bound preferentially to domain IV, as shown in two distinct views (Figure 5B). The localization of Spt20 to a site apart from the focal center of the structure offers an explanation for the severe reduction, but not complete loss, of several proteins in SAGA in an *spt20*Δ mutant (Wu and Winston, 2002). This is in contrast to the *ada1*Δ mutant described above, which lacks two centrally located Ada1 molecules and retains a much smaller, partial complex.

Mapping of SAGA Subunits that Regulate Transcription: Spt3 and Gcn5

SAGA possesses a number of subunits that regulate different aspects of transcription. One catalytic activity of SAGA is provided by the histone acetyltransferase Gcn5. In addition, the Spt3 subunit has been shown by both genetic and biochemical methods to regulate TBP interactions with the promoter. Gcn5 and Spt3 have been shown to regulate distinct sets of genes (Lee et al., 2000; Roberts and Winston, 1997; Sterner et al., 1999). To understand the organization of these transcriptional regulators in SAGA, we mapped their loca-

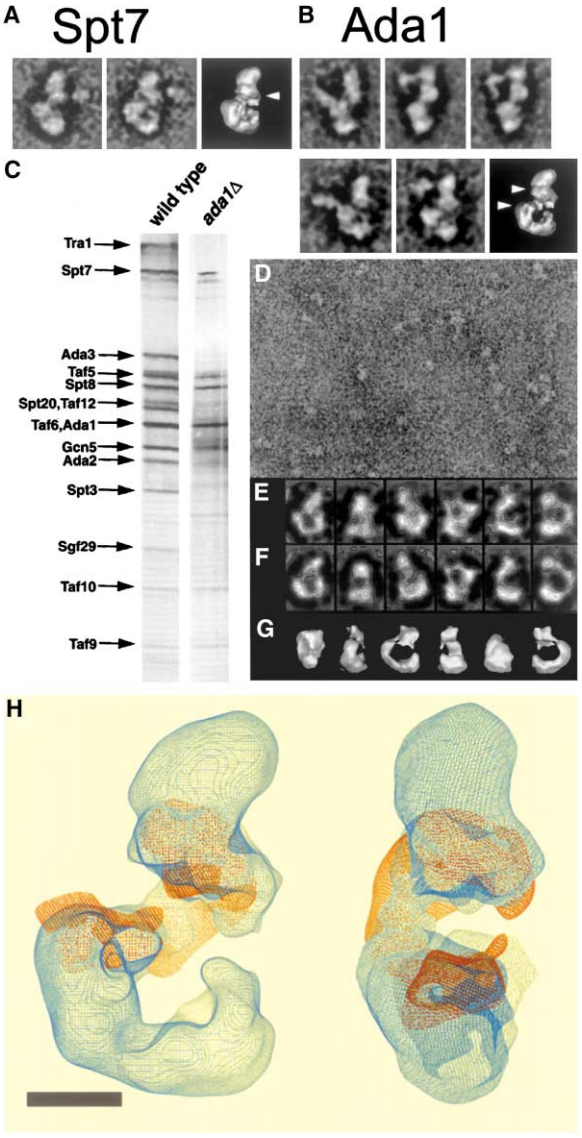

Figure 4. Mapping of the Histone Fold Domain-Containing Core Components Spt7 and Ada1 and Analysis of the *ada1*Δ Mutant

(A) Mapping of Spt7 by using either the CBP moiety fused to the C terminus of Spt7 and a streptavidin-coupled, biotinylated calmodulin as probe (left panel) or a HA-specific antibody to label the N-terminally HA-tagged Spt7 subunit (center panel). Both probes bind to a single site in domain III (arrows in the 3D model in the right panel).

(B) Mapping of Ada1 with a subunit-specific polyclonal antibody. Two distinct SAGA views were analyzed (upper and lower panels, respectively) and specific labeled sites were identified on two sites as shown by average images of SAGA molecules labeled in domains II and III (left and central panels, respectively). The upper right panel shows that a single antibody can label two sites. The lower right panel show a surface representations of the 3D model of SAGA on which the antibody binding sites are indicated by arrowheads.

(C) Silver stain of SAGA purified from wild-type (FY2031) and *ada1*Δ (FY2035) strains.

(D) Electron micrograph of SAGA *ada1*Δ molecules adsorbed on a carbon film and negatively stained with uranyl acetate.

(E) Gallery of the most representative *ada1*Δ mutant views obtained upon averaging aligned images clustered into homogeneous classes. The stain-excluding protein densities are outlined by contours of equal density. The six views correspond to different orientations of the molecule.

tions. The position of Spt3 in SAGA was determined using HA-tagged Spt3 with an HA-specific antibody. The analysis showed a specific antibody binding to domain V in SAGA, indicating that Spt3 is located in this flexible part of the molecule (Figure 5C). This position for the Spt3 subunit in or near domain V identifies a potential TBP interaction module in the structure of SAGA. The histone acetyltranferase subunit Gcn5 was mapped using a Gcn5-specific antibody, and the analysis of 1676 labeled complexes showed, in two different views, that the antibodies bound to domain III in SAGA (Figure 5D). The Gcn5 subunit thus resides in the vicinity of the Taf subcomplex. This position for Gcn5 is intriguing, as it places the bromodomains in Spt7 and Gcn5, which interact with acetylated lysine in histone tails, in close proximity. It also separates the histone acetyltransferase activity of SAGA from the functionally distinct Spt3 subunit (Figure 5E).

Discussion

This study provides the first low-resolution 3D model of the *S. cerevisiae* SAGA coactivator complex, maps the positions of key subunits, and offers insight into the functional organization of the complex. As depicted in Figure 6, SAGA is arranged into five distinct domains that appear to have specialized functions. The central domains II, III, and IV contain the Taf subunits that are shared with TFIID, and they are believed to play primarily an architectural role. The SAGA-specific structural components Spt7, Spt20, and Ada1 are also located within these regions. Domains I and V are involved in transcriptional regulatory functions as domain I consists mainly of the Tra1 protein, required for interaction with activators, and the flexible domain V contains the TBP-regulating proteins Spt3. The histone acetyltransferase Gcn5 is located in domain III. Overall, the organization of SAGA components into structural modules reflects their distinct functional roles.

The purified SAGA preparations reproducibly contain a large fraction of elongated particles that were shown to disappear when a deletion mutation is introduced into *ADA1* and are therefore likely to represent the particles related to the biological activity. Smaller particles were also observed that most likely correspond to degradation products or to contaminants. In contrast to the elongated particles, these complexes are heterogeneous in size and too small to contain all the known SAGA subunits. It cannot be excluded that the SAGA preparation contains a minor subpopulation of Spt7-containing complexes that were not further analyzed. It

(F) Reprojections of the calculated 3D model of the *ada1*Δ mutant along the same directions of the experimental views shown in Figure 4E, illustrating the similarity with the original views.

(G) Three-dimensional model of the *ada1*Δ mutant particles showing a three-lobed architecture.

(H) Superposition of the 3D models obtained from the *ada1*Δ mutant particles (orange) and from the wild-type SAGA particles (turquoise) that maximizes the fit between the two volumes and is consistent with the position of the Ada1 subunits as determined by immunoelectron microscopy. The bar represents 38 nm in (A) and (B), 112 nm in (D), 29 nm in (E–G), and 6.8 nm in (H).

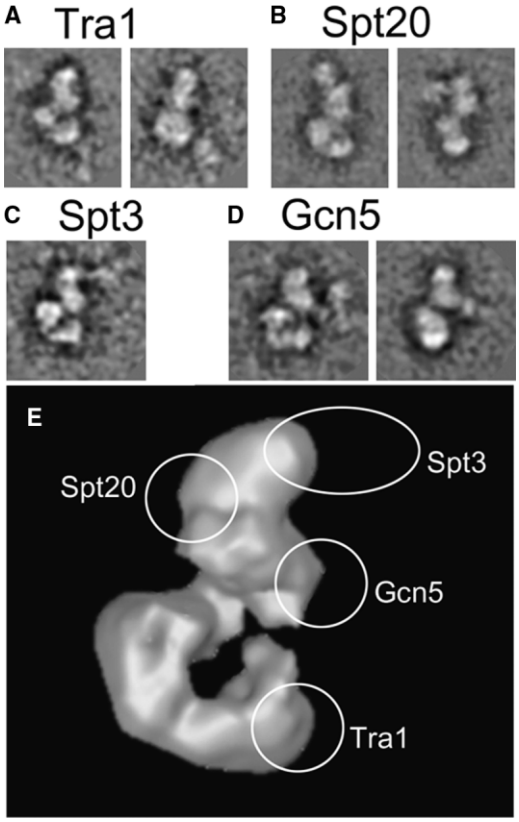

Figure 5. Immunolabeling of Spt20 and Tra1, Two Core Components of the SAGA Complex, as well as Spt3 and Gcn5 within SAGA

(A) Mapping of the myc-tagged Tra1 subunit in a wild-type strain (L1065) with a myc-specific antibody. A specific labeled site was identified in domain I in two distinct SAGA views (left and right panels).

(B) Mapping of Spt20 with a subunit-specific polyclonal antibody on two distinct views of the SAGA complex.

(C) Mapping of the HA-tagged Spt3 subunit in a wild-type strain (FY2267) with HA-specific antibody. Spt3 is located in or near the variable domain V in SAGA.

(D) Mapping of the Gcn5 subunit with a Gcn5-specific antibody. A specific labeled site was identified in domain III in two distinct SAGA views.

(E) Schematic location of the labeled subunits within the 3D model of SAGA.

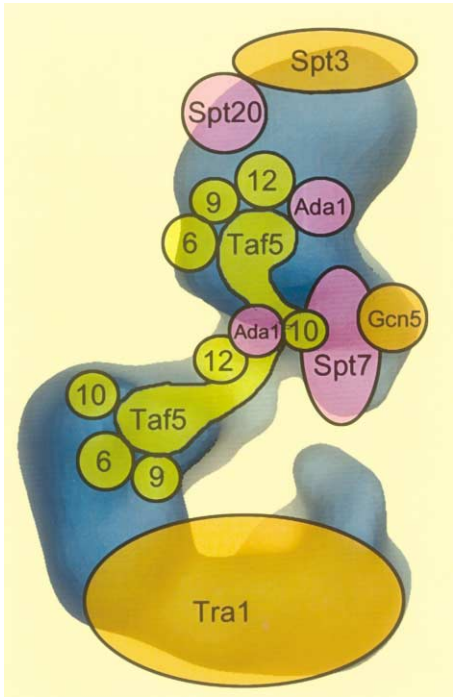

Figure 6. Schematic Representation of the Localization of the SAGA Subunits on the 3D Model of the Complex

The Taf subunits are represented in yellow and, except for Taf5, their names were shortened to their identification number (e.g., 10 for Taf10). The extended shape of Taf5 and the positions of Taf9 and Taf12 were inferred from previous results on TFIID (Leurent et al., 2002, 2004), assuming that the position and subunit stoichiometry of the Taf substructure is conserved. SAGA-specific histone fold containing and architectural subunits are represented in purple, whereas SAGA subunits involved in various aspects of transcriptional regulation are represented in orange.

is unlikely that a particularly fragile subdomain systematically falls off the bona fide SAGA complex during specimen preparation, as was observed in some complexes for domain V. In that situation both small and elongated particles should be observed with the same frequency, which is not the case.

The structure of SAGA is strikingly similar to that of the human TFTC complex. This conservation of structure is consistent with previous findings that the components of the two complexes are conserved between *S. cerevisiae* and humans (Brand et al., 1999b; Martinez et al., 1998, 2001; Ogryzko et al., 1998). Although these complexes share a central structure, there are differences in the variable regions in SAGA and TFTC that may be attributed to the unique subunits in each complex. For example, while TFTC contains PAF65β, Taf2, and Taf4, those components are not conserved in SAGA (Brand et al., 1999b). Moreover, some of the subunits common to both TFTC and SAGA, including Spt7, are not well conserved between humans and yeast (Martinez et al., 2001). Aside from these differences, the similarity in the structures of TFTC and SAGA likely reflects a common mechanism for regulating transcription.

Insight into the core structure of SAGA was provided by comparing the positions of the Taf subunits and their interaction partners in SAGA and in TFIID. The mapping of Taf5, Taf6, and Taf10 and subsequent alignment of the structures of TFIID and SAGA reveal a similar spatial distribution of the Tafs. In Figure 6, we have noted the positions of the Tafs and extrapolated the distributions of Taf9 and Taf12 from their location in TFIID (Leurent et al., 2002). A similar extrapolation was made for Taf5 for which a 2-fold stoichiometry was determined in yeast TFIID from electron microscopy and biochemical experiments (Leurent et al., 2004; Sanders et al., 2002). In yTFIID, the N and C termini of Taf5 were found in different lobes, but the two N termini were located in the same lobe and were not resolved by the mapping. The same situation may exist in SAGA where a single labeled site was found with the antibody directed against the N terminus of Taf5. Our data suggest the existence of a Taf substructure that serves as a scaffold for SAGA assembly. In TFIID, this substructure contains Taf heterodimer

pairs that have been shown to interact via their histone fold domains, including Taf4-Taf12, Taf6-Taf9, and Taf10-Taf3/Taf8 (Gangloff et al., 2000, 2001; Hoffmann et al., 1996; Xie et al., 1996). Some of these Tafs can also interact with SAGA components, forming Taf10-Spt7 and Taf12-Ada1 heterodimers. Our data support these associations since the HFD-containing subunits Ada1 and Spt7 are positioned in close proximity to their Taf partners where they could form a SAGA-specific interface with the Tafs. One uncertainty in our analysis of SAGA is the stoichiometry of Taf10. Taf10 was clearly located at two distinct places in TFIID, a result confirmed by coimmunoprecipitation experiments and by the quantitation of SDS-PAGE bands (Leurent et al., 2004; Sanders et al., 2002). We failed to demonstrate that in SAGA Taf10 was also present in two distinct locations because the preferential view obtained in the immunolabeling experiments showed an internal symmetry. Moreover, immunoprecipitation experiments did not show a strong coprecipitation of Taf10 and its tagged version (data not shown), and the location of its heterodimerization partner Spt7 also showed a single location in SAGA. Thus, we cannot rule out the possibility that the stoichiometry of Taf10 may be different in SAGA than in TFIID.

The positions of SAGA components that are involved in transcriptional regulation, Spt3, Gcn5, and Tra1, suggest a modular organization that reflects their distinct regulatory activities. Strikingly, each of these three functions is located in a distinct domain. Several studies have suggested that Spt3 plays related roles in transcription initiation by regulating the TBP-TATA interaction (Barbaric et al., 2003; Belotserkovskaya et al., 2000; Bhaumik and Green, 2001; Eisenmann et al., 1992; Larschan and Winston, 2001; Yu et al., 2003). Our results show that Spt3 forms a part of domain V, potentially constituting a TBP regulatory module in SAGA. The histone acetyltransferase activity provided by Gcn5 is located in domain III, spatially segregated from Spt3. Domain III may also contain Ada2 and Ada3, both of which have been shown to be required for the specific nucleosomal HAT activity of Gcn5 (Balasubramanian et al., 2001; Sterner et al., 2002). In addition, the localization of Spt7 and Gcn5 to adjacent positions places two bromodomain motifs in close proximity, allowing for multiple interactions with histone tails. The positions of these components could point to a chromatin-interacting module in SAGA that associates with and modifies nucleosomes. Interestingly, the size of the large cleft formed by lobes I, II, and III exactly accommodates the dimensions of a 10 $\times$ 4.5 nm, disk-shaped nucleosome (see Supplemental Data at http://www.molecule.org/cgi/content/full/15/2/199/DC1). This would place the Gcn5 subunit in the appropriate position to modify histones.

Our results offer a description of the molecular architecture of the SAGA complex and suggest a direction for future studies. The core of SAGA, containing the Taf substructure, is surrounded by three domains responsible for distinct functions: activator binding, histone acetylation, and TBP regulation. This structural organization illustrates an underlying principle of modularity that may be extended to our understanding of other multifunctional transcription complexes. Additional structural data examining the interactions of SAGA with activators or general transcription factors may uncover more subtle details that are relevant for SAGA function. In the case of the CRSP coactivator, for instance, binding to an activator or to the C-terminal domain of RNA polymerase II causes distinct conformational changes (Naar et al., 2002; Taatjes et al., 2002). These interaction-induced changes may be important for activating specific target genes. Further structural analysis of SAGA bound to a chromatin array would reveal a more accurate view of the contacts between SAGA and the promoter and provide additional details for its mechanism of function.

Experimental Procedures

S. cerevisiae Strains, Cell Transformation, and *S. cerevisiae* SAGA Purification

The following *S. cerevisiae* strains, all descended from a *GAL2*$^+$ derivative of S288C (Winston et al., 1995), were used in this study: FY2031 (*MAT***a** *HA-SPT7-TAP::TRP1 ura3*Δ*0 leu2*Δ*1 trp1*Δ*63 his4-917*δ *lys2-173R2*); FY2035 (*MAT***a** *HA-SPT7-TAP::TRP1 ura3*Δ*0 leu2*Δ*1 trp1*Δ*63 his3*Δ*200 ada1*Δ*::HIS3 lys2-173R2 his4-917*δ); FY2267 (*MAT***a** *SPT7-TAP::TRP1 HA-SPT3 ura3*Δ*0 leu2*Δ*0 his4-917*δ *lys2-173R2*), and L1065 (*MAT***a** *SPT7-TAP::TRP1 trp1*Δ*63 lys2-173R2 MYC-TRA1 leu2*Δ*0 ura3*Δ*0*). The *ada1*Δ allele used, as well as *HA-SPT3*, *HA-SPT7-TAP*, and *TRA1-MYC*, have been described previously (Hall and Struhl, 2002; Larschan and Winston, 2001; Sterner et al., 1999; Wu and Winston, 2002). Standard methods for mating, sporulation, transformations, and tetrad analysis were used, and all media were prepared as described (Rose et al., 1990).

The protocol used to purify SAGA containing TAP-tagged Spt7 has been described (Wu and Winston, 2002) except for the calmodulin-binding and elution buffers that contained only 0.02% NP-40. SAGA fractions were concentrated using Centricon-10 columns to 40 μl for each purification from 2 liters of yeast grown to $\sim$2 $\times$ 10^7 cells/ml. Silver staining was performed according to the protocol from the Yeast Resource Center at the University of Washington (http://depts.washington.edu/yeastrc/ms_silver.htm).

Electron Microscopy and Image Processing

The purified SAGA fractions were diluted to a concentration of 20 μg/ml in 20 mM Tris-HCl (pH 7.4), 150 mM NaCl, and 20% glycerol. 10 μl of this preparation was placed on a 10 nm thick carbon film previously treated by a glow discharge in air. After 2 min of adsorption, the grid was negatively stained with a 2% (w/v) uranyl acetate solution. The images were formed on a Philips CM120 Transmission Electron Microscope operating at 100 kV with a LaB6 filament. Areas covered with individual molecules were recorded at a magnification of 35,000$\times$ on a Pelletier cooled slow scan CCD camera (Model 794, Gatan, Pleasanton). The image processing was performed using the IMAGIC software package (van Heel et al. (1996) (Image Science Software, Berlin, Germany). The images of negatively stained SAGA molecules were floated, normalized, band-pass filtered, and centered onto a rotationally averaged summation of all images. The images were then analyzed by using multivariate statistical methods and hierarchic ascendant classification to identify characteristic molecular views to be used as alignment references. The 3D model of TFTC was not used as alignment reference to avoid any bias during this step. After three alignment/classification cycles the image partition was stable and the angular assignment of the class averages was performed using the angular reconstitution method (van Heel, 1988). At this stage the 3D model of human TFTC (Brand et al., 1999a) was used to determine the viewing directions of the class averages by sinogram correlation functions. The class averages were combined by back projection methods, and projections of the resulting 3D model were used as references for two additional alignment/classification steps. The resolution of the final reconstruction was estimated from the Fourier shell correlation function obtained by comparing two independent reconstructions, generated by splitting randomly the data set in half, according to the 0.5 cutoff in the Fourier shell correlation curve (0.5 FSC criterion) and the intersection point of the 3σ curve with the FSC curve (3σ criterion)

(van Heel, 1987). Docking and color figures were performed by using the program Dino (Dino: Visualizing Structural Biology, http://cobra.mih.unibas.ch/dino)

Immunolabeling

Specific polyclonal rabbit antibodies (pAbs) recognizing yTaf5, yTaf6, and yTaf10 were generated, purified, and characterized as described previously (Leurent et al., 2004; Sanders et al., 1999). The characterization of antibodies for Spt20 and Ada1 was described (Grant et al., 1997; Horiuchi et al., 1997; Roberts and Winston, 1996). For use in immunolabeling experiments, these antibodies were purified using Protein G Fastflow from Pharmacia and stored at a concentration of 100 μg/ml.

For immunoelectron microscopy a 3- to 5-fold molar excess of antibodies was incubated 30 min at 20°C with purified SAGA at a final protein concentration of 20 μg/ml. The statistical analysis of the immune complexes, necessary to validate the binding specificity was performed as described previously (Leurent et al., 2002). Briefly, images of SAGA molecules putatively labeled by an antibody were collected, and the orientation of each SAGA molecule was attributed to one out of 66 equally spaced views generated from the 3D model. The classes containing the largest number of particles were further analyzed to determine the antibody binding specificity which was evaluated by dividing the contour of the molecular view into eight equivalent sectors and plotting the antibody binding site of each labeled complex into one of these sectors. The binding was judged as specific when one or more sectors bound antibodies significantly more frequently (average $+ 3\sigma$) than the average binding frequency of background sectors.

Calmodulin Probe

In order to locate Spt7, we took advantage of the calmodulin binding peptide that remains on the TAP-tagged subunit after TEV cleavage. Calmodulin was biotinylated, gel filtrated to remove the excess of biotinylation agent, and reacted with equimolar amounts of streptavidin. This probe was examined by EM to show that there was no excess of calmodulin in the background. The experiment also showed that the streptavidin molecules are decorated, probably by calmodulin molecules. The probe was incubated with SAGA CBP tagged on Spt7, in the presence of 10 mM $CaCl_2$.

Acknowledgments

We are grateful to Tony Weil for providing antibodies to the Taf10, Taf6, and Gcn5; Làszlò Tora for antibodies against Taf5; and Dan Hall and Kevin Struhl for a strain containing the Tra1-Myc allele. We thank David Hess for the suggestion to use the calmodulin binding peptide in the TAP tag for subunit labeling and M. Schatz (Image Science Software, Berlin, Germany) for customizing the IMAGIC software package. P.-Y.J.W. was supported by a predoctoral fellowship from the Howard Hughes Medical Institute. This work was supported by the Institut National de la Santé et de la Recherche Médicale, the Centre National pour la Recherche Scientifique, the Hôpital Universitaire de Strasbourg (HUS), the Association pour la Recherche sur le Cancer, and the European Union grant RTN2-2001-00026 to P.S. This work was also supported by National Institutes of Health grant GM45720 to F.W.

Received: January 27, 2004
Revised: May 7, 2004
Accepted: May 18, 2004
Published: July 22, 2004

References

Allard, S., Utley, R.T., Savard, J., Clarke, A., Grant, P., Brandl, C.J., Pillus, L., Workman, J.L., and Cote, J. (1999). NuA4, an essential transcription adaptor/histone H4 acetyltransferase complex containing Esa1p and the ATM-related cofactor Tra1p. EMBO J. *18*, 5108–5119.

Balasubramanian, R., Pray-Grant, M.G., Selleck, W., Grant, P.A., and Tan, S. (2001). Role of the Ada2 and Ada3 transcriptional coactivators in histone acetylation. J. Biol. Chem. *31*, 7989–7995.

Barbaric, S., Reinke, H., and Horz, W. (2003). Multiple mechanistically distinct functions of SAGA at the PHO5 promoter. Mol. Cell. Biol. *23*, 3468–3476.

Belotserkovskaya, R., Sterner, D.E., Deng, M., Sayre, M.H., Lieberman, P.M., and Berger, S.L. (2000). Inhibition of TATA-binding protein function by SAGA subunits Spt3 and Spt8 at Gcn4-activated promoters. Mol. Cell. Biol. *20*, 634–647.

Bhaumik, S.R., and Green, M.R. (2001). SAGA is an essential in vivo target of the yeast acidic activator Gal4p. Genes Dev. *15*, 1935–1945.

Bhaumik, S.R., Raha, T., Aiello, D.P., and Green, M.R. (2004). In vivo target of a transcriptional activator revealed by fluorescence resonance energy transfer. Genes Dev. *18*, 333–343.

Brand, M., Leurent, C., Mallouh, V., Tora, L., and Schultz, P. (1999a). Three-dimensional structures of the TAFII-containing complexes TFIID and TFTC. Science *286*, 2151–2153.

Brand, M., Yamamoto, K., Staub, A., and Tora, L. (1999b). Identification of TATA-binding protein-free TAFII-containing complex subunits suggests a role in nucleosome acetylation and signal transduction. J. Biol. Chem. *274*, 18285–18289.

Brown, C.E., Howe, L., Sousa, K., Alley, S.C., Carrozza, M.J., Tan, S., and Workman, J.L. (2001). Recruitment of HAT complexes by direct activator interactions with the ATM-related Tra1 subunit. Science *292*, 2333–2337.

Brownell, J.E., Zhou, J., Ranalli, T., Kobayashi, R., Edmondson, D.G., Roth, S.Y., and Allis, C.D. (1996). Tetrahymena histone acetyltransferase A: a homolog to yeast Gcn5p linking histone acetylation to gene activation. Cell *84*, 843–851.

Cosma, M.P. (2002). Ordered recruitment: gene-specific mechanism of transcription activation. Mol. Cell *10*, 227–236.

Durso, R.J., Fisher, A.K., Albright-Frey, T.J., and Reese, J.C. (2001). Analysis of TAF90 mutants displaying allele-specific and broad defects in transcription. Mol. Cell. Biol. *21*, 7331–7344.

Eisenmann, D.M., Arndt, K.M., Ricupero, S.L., Rooney, J.W., and Winston, F. (1992). SPT3 interacts with TFIID to allow normal transcription in Saccharomyces cerevisiae. Genes Dev. *6*, 1319–1331.

Gangloff, Y.G., Werten, S., Romier, C., Carre, L., Poch, O., Moras, D., and Davidson, I. (2000). The human TFIID components TAF(II)135 and TAF(II)20 and the yeast SAGA components ADA1 and TAF(II)68 heterodimerize to form histone-like pairs. Mol. Cell. Biol. *20*, 340–351.

Gangloff, Y.G., Sanders, S.L., Romier, C., Kirschner, D., Weil, P.A., Tora, L., and Davidson, I. (2001). Histone folds mediate selective heterodimerization of yeast TAF(II)25 with TFIID components yTAF(II)47 and yTAF(II)65 and with SAGA component ySPT7. Mol. Cell. Biol. *21*, 1841–1853.

Grant, P.A., Duggan, L., Cote, J., Roberts, S.M., Brownell, J.E., Candau, R., Ohba, R., Owen-Hughes, T., Allis, C.D., Winston, F., et al. (1997). Yeast Gcn5 functions in two multisubunit complexes to acetylate nucleosomal histones: characterization of an Ada complex and the SAGA (Spt/Ada) complex. Genes Dev. *11*, 1640–1650.

Grant, P.A., Schieltz, D., Pray-Grant, M.G., Steger, D.J., Reese, J.C., Yates, J.R., III, and Workman, J.L. (1998a). A subset of TAF(II)s are integral components of the SAGA complex required for nucleosome acetylation and transcriptional stimulation. Cell *94*, 45–53.

Grant, P.A., Schieltz, D., Pray-Grant, M.G., Yates, J.R., III, and Workman, J.L. (1998b). The ATM-related cofactor Tra1 is a component of the purified SAGA complex. Mol. Cell *2*, 863–867.

Grant, P.A., Eberharter, A., John, S., Cook, R.G., Turner, B.M., and Workman, J.L. (1999). Expanded lysine acetylation specificity of Gcn5 in native complexes. J. Biol. Chem. *274*, 5895–5900.

Hall, D.B., and Struhl, K. (2002). The VP16 activation domain interacts with multiple transcriptional components as determined by protein-protein cross-linking in vivo. J. Biol. Chem. *277*, 46043–46050.

Hoffmann, A., Chiang, C.M., Oelgeschlager, T., Xie, X., Burley, S.K., Nakatani, Y., and Roeder, R.G. (1996). A histone octamer-like structure within TFIID. Nature *380*, 356–359.

Horiuchi, J., Silverman, N., Pina, B., Marcus, G.A., and Guarente, L. (1997). ADA1, a novel component of the ADA/GCN5 complex, has

broader effects than GCN5, ADA2, or ADA3. Mol. Cell. Biol. *17*, 3220–3228.

Kirschner, D.B., vom Baur, E., Thibault, C., Sanders, S.L., Gangloff, Y.G., Davidson, I., Weil, P.A., and Tora, L. (2002). Distinct mutations in yeast TAF(II)25 differentially affect the composition of TFIID and SAGA complexes as well as global gene expression patterns. Mol. Cell. Biol. *22*, 3178–3193.

Klein, J., Nolden, M., Sanders, S.L., Kirchner, J., Weil, P.A., and Melcher, K. (2003). Use of a genetically introduced cross-linker to identify interaction sites of acidic activators within native transcription factor IID and SAGA. J. Biol. Chem. *278*, 6779–6786.

Larschan, E., and Winston, F. (2001). The S. cerevisiae SAGA complex functions in vivo as a coactivator for transcriptional activation by Gal4. Genes Dev. *15*, 1946–1956.

Lee, T.I., Causton, H.C., Holstege, F.C.P., Shen, W.-C., Hannett, N., Jennings, E.G., Winston, F., Green, M.R., and Young, R.A. (2000). Redundant roles for the TFIID and SAGA complexes in global transcription. Nature *405*, 701–704.

Leurent, C., Sanders, S., Ruhlmann, C., Mallouh, V., Weil, P.A., Kirschner, D.B., Tora, L., and Schultz, P. (2002). Mapping histone fold TAFs within yeast TFIID. EMBO J. *21*, 3424–3433.

Leurent, C., Sanders, S., Demeny, M.A., Garbett, K.A., Ruhlmann, C., Weil, P.A., Tora, L., and Schultz, P. (2004). Mapping key functional sites within yeast TFIID. EMBO J. *23*, 719–727.

Martinez, E., Kundu, T.K., Fu, J., and Roeder, R.G. (1998). A human SPT3-TAFII31-GCN5-L acetylase complex distinct from transcription factor IID. J. Biol. Chem. *273*, 23781–23785.

Martinez, E., Palhan, V.B., Tjernberg, A., Lymar, E.S., Gamper, A.M., Kundu, T.K., Chait, B.T., and Roeder, R.G. (2001). Human STAGA complex is a chromatin-acetylating transcription coactivator that interacts with pre-mRNA splicing and DNA damage- binding factors in vivo. Mol. Cell. Biol. *21*, 6782–6795.

Naar, A.M., Taatjes, D.J., Zhai, W., Nogales, E., and Tjian, R. (2002). Human CRSP interacts with RNA polymerase II CTD and adopts a specific CTD-bound conformation. Genes Dev. *16*, 1339–1344.

Ogryzko, V.V., Kotani, T., Zhang, X., Schlitz, R.L., Howard, T., Yang, X.J., Howard, B.H., Qin, J., and Nakatani, Y. (1998). Histone-like TAFs within the PCAF histone acetylase complex. Cell *94*, 35–44.

Reese, J.C., Zhang, Z., and Kurpad, H. (2000). Identification of a yeast transcription factor IID subunit, TSG2/TAF48. J. Biol. Chem. *275*, 17391–17398.

Roberts, S.M., and Winston, F. (1996). SPT20/ADA5 encodes a novel protein functionally related to the TATA-binding protein and important for transcription in Saccharomyces cerevisiae. Mol. Cell. Biol. *16*, 3206–3213.

Roberts, S.M., and Winston, F. (1997). Essential functional interactions of SAGA, a Saccharomyces cerevisiae complex of Spt, Ada, and Gcn5 proteins, with the Snf/Swi and Srb/mediator complexes. Genetics *147*, 451–465.

Rose, M.D., Winston, F., and Hieter, P. (1990). Methods in Yeast Genetics: A Laboratory Course Manual (Cold Spring Harbor, NY: Cold Spring Harbor Laboratory Press).

Roth, S.Y., Denu, J.M., and Allis, C.D. (2001). Histone acetyltransferases. Annu. Rev. Biochem. *70*, 81–120.

Saleh, A., Schieltz, D., Ting, N., McMahon, S.B., Litchfield, D.W., Yates, J.R., III, Lees-Miller, S.P., Cole, M.D., and Brandl, C.J. (1998). Tra1p is a component of the yeast Ada.Spt transcriptional regulatory complexes. J. Biol. Chem. *273*, 26559–26565.

Sanders, S.L., Klebanow, E.R., and Weil, P.A. (1999). TAF25p, a non-histone-like subunit of TFIID and SAGA complexes, is essential for total mRNA gene transcription in vivo. J. Biol. Chem. *274*, 18847–18850.

Sanders, S.L., Jennings, J., Canutescu, A., Link, A.J., and Weil, P.A. (2002). Proteomics of the eukaryotic transcription machinery: identification of proteins associated with components of yeast TFIID by multidimensional mass spectrometry. Mol. Cell. Biol. *22*, 4723–4738.

Selleck, W., Howley, R., Fang, Q., Podolny, V., Fried, M.G., Buratowski, S., and Tan, S. (2001). A histone fold TAF octamer within the yeast TFIID transcriptional coactivator. Nat. Struct. Biol. *8*, 695–700.

Sterner, D.E., Grant, P.A., Roberts, S.M., Duggan, L.J., Belotserkovskaya, R., Pacella, L.A., Winston, F., Workman, J.L., and Berger, S.L. (1999). Functional organization of the yeast SAGA complex: distinct components involved in structural integrity, nucleosome acetylation, and TATA- binding protein interaction. Mol. Cell. Biol. *19*, 86–98.

Sterner, D.E., Wang, X., Bloom, M.H., and Berger, S.L. (2002). The SANT domain of Ada2 is required for normal acetylation of histones by the yeast SAGA complex. J. Biol. Chem. *2*, 8178–8186.

Taatjes, D.J., Naar, A.M., Andel, F., III, Nogales, E., and Tjian, R. (2002). Structure, function, and activator-induced conformations of the CRSP coactivator. Science *295*, 1058–1062.

van Heel, M. (1987). Similarity measures between images. Ultramicroscopy *21*, 95–100.

van Heel, M. (1988). Angular reconstitution: a-posteriori assignment of projection directions for 3D reconstruction. Ultramicroscopy *21*, 111–124.

van Heel, M., Harauz, G., and Orlova, E.V. (1996). A new generation of the IMAGIC image processing system. J. Struct. Biol. *116*, 17–24.

Winston, F., Dollard, C., and Ricupero-Hovasse, S.L. (1995). Construction of a set of convenient Saccharomyces cerevisiae strains that are isogenic to S288C. Yeast *11*, 53–55.

Wu, P.Y., and Winston, F. (2002). Analysis of Spt7 function in the Saccharomyces cerevisiae SAGA coactivator complex. Mol. Cell. Biol. *22*, 5367–5379.

Xie, X., Kokubo, T., Cohen, S.L., Mirza, U.A., Hoffmann, A., Chait, B.T., Roeder, R.G., Nakatani, Y., and Burley, S.K. (1996). Structural similarity between TAFs and the heterotetrameric core of the histone octamer. Nature *380*, 316–322.

Yu, Y., Eriksson, P., Bhoite, L.I., and Stillman, D.J. (2003). Regulation of TATA-binding protein binding by the SAGA complex and the Nhp6 high-mobility group protein. Mol. Cell. Biol. *23*, 1910–1921.